Coral Reefs (2004) 23: 281–296
DOI 10.1007/s00338-004-0378-x

REPORT

C. Pinazo · S. Bujan · P. Douillet · R. Fichez
C. Grenz · A. Maurin

Impact of wind and freshwater inputs on phytoplankton biomass in the coral reef lagoon of New Caledonia during the summer cyclonic period: a coupled three-dimensional biogeochemical modeling approach

Received: 1 August 2002 / Accepted: 15 April 2003 / Published online: 13 May 2004

Abstract A coupled three-dimensional physical-biological model was developed in order to simulate the ecological functioning and potential impacts of land-derived inputs in the southwest lagoon of New Caledonia. This model considered pelagic biogeochemical cycling of organic matter, taking into account advection and diffusion processes driven mainly by local wind fields and freshwater discharges. Modeled phytoplankton dynamic were strongly correlated with both freshwater nutrient inputs and wind-driven hydrodynamic processes, the latter resulting in a large input of oceanic water from the southeast part of the lagoon under trade wind conditions. In situ data obtained during the summer (January 1998) under trade wind conditions supported predicted concentration gradients along several coast to reef transects and provided a validation of the coupled physical-biogeochemical model. An additional sensitivity analysis showed that the alteration of the biogeochemical parameters did not strongly affect the results of the model. Freshwater inputs of nutrients were simulated using a realistic scenario corresponding to the summer rainy season of 1997–1998 in New Caledonia. Despite occasional flooding events from the main rivers considered in these simulations, no significant meso-scale phytoplankton bloom was identified. Hydrodynamically driven dispersion and rapid uptake of nutrients by phytoplankton were sufficient to spatially constrain the impact of river inputs and maintain oligotrophic conditions. The fine spatial grid of our three-dimensional model demonstrated that eutrophication in the southwest lagoon of New Caledonia is confined to the most restricted coastal embayments, while most of the lagoon experiences sustained oligotrophic conditions.

Keywords Coupled physical-biological three-dimensional modeling · Biogeochemistry · Ecosystem · Phytoplankton · Lagoon · New Caledonia

C. Pinazo (✉) · S. Bujan · C. Grenz · A. Maurin
Station Marine d'Endoume (Bat 4),
Centre d'Oceanologie de Marseille,
Chemin de la Batterie des Lions,
13007 Marseille, France
E-mail: pinazo@com.univ-mrs.fr

P. Douillet · R. Fichez
Institut de Recherche pour le Developpement (IRD),
BP A 5 Noumea, New Caledonia, 98848, Canada

Introduction

The New Caledonia Reef is the second widest tropical reef system in the world after the Australian Great Barrier Reef. This single, continuous barrier reef surrounding New Caledonia's main island is 1,100-km long and delimits a lagoon area of 23,400 km^2. Terrigenous inputs of either natural or anthropogenic origin is perceived as one of the main structuring factors in this enclosed system (Labrosse et al. 2000). A coupled physical-biological, three-dimensional modeling approach was used in order to gain better insights into the ecological functioning and potential impact of land-derived inputs in this coral reef environment.

The use of models to simulate marine coastal environments has increased significantly during the past 25 yr in parallel with the availability of powerful computing tools. Most of the early models focused on the first levels of the pelagos (nutrients, phytoplankton) under steady-state conditions (Steele 1962; Billen 1978). Deterministic approaches were progressively used to model time-varying conditions related to abiotic forcings (hydrodynamics, meteorology, air-water exchanges, etc.), and to introduce more precise ecological processes in NPZD models (Billen and Lancelot 1988; Fasham et al. 1990).

Two main types of models are used in marine biogeochemistry:

- Box models representing ecosystems as homogeneous water bodies where hydrodynamic processes are simplified to avoid extensive calculation. This allows relatively complex description of the biochemical processes.
- Numerical models with fine resolution of one to three dimensions, representing ecosystems as spatially heterogeneous and needing strong computing technology with considerable capacity of storage space, a large number of grid points, and small time steps. Biogeochemical processes are less detailed than in box models, and the number of state variables is usually restricted.

Modeling is seldom undertaken in tropical coastal systems. Based on the high biodiversity of these systems and using trophic mass balance, the Ecopath model (Atkinson and Grigg 1984; Christensen and Pauly 1992) provides interesting and complex results for food-webs in tropical lagoons (Guarin 1991; Arias-Gonzales 1993). Inverse modeling approaches have been used to simulate processes such as the impact of fisheries (McClanahan 1995) or the influence of aquaculture (Niquil et al. 1998) in tropical lagoons.

Deterministic, fine spatial-grid models have recently been applied in temperate environments (Aksnes et al. 1995; ; Skogen et al. 1995; Gregoire et al. 1998; Tusseau-Vuillemin et al. 1998; Zavatarelli et al. 2000; Pinazo et al. 2001; ; Skliris et al. 2001), but similar approaches coupling biogeochemical and hydrodynamic processes in an entire tropical coastal ecosystem are less common. The development of hydrodynamic models is a limiting perquisite to the development of coupled biogeochemical modeling. The increased use of hydrodynamic models for tropical coastal areas (Wolanski 1994; Tartinville et al. 1997; Douillet 1998) provides physical background to explain biological processes on a dynamic basis. Considering the paucity of extensive biogeochemical observations in coral reef lagoons, the multidisciplinary oceanographic study conducted by IRD (Institut de Recherche pour le Developpement) on the New Caledonia lagoon around Noumea provided a favorable context to initiate biogeochemical modeling studies.

The first modeling part of this program developed a box model to produce multiyear simulations with daily time steps (Bujan et al. 2000). No seasonality was demonstrated in the modeled dynamics of nutrients and phytoplankton. Long-term simulations showed the capacity of the system to absorb significant terrigenous and anthropogenic inputs, while maintaining oligotrophic conditions in the lagoon (Bujan 2000; Bujan et al. 2000).

In the work presented here, we took the next step in modeling by using a fine-resolution model, coupling biogeochemical fluxes with hydrodynamic processes. This three-dimensional, coupled physical-biological model enabled us to focus on the dynamics of the pelagic system near the coast during the summer period when terrestrial inputs and probability of eutrophication is highest. Specifically, we present realistic scenarios of wind forcing in order to highlight the interactions between seasonal freshwater inputs and wind-related hydrodynamics on phytoplankton biomass in the lagoon of New Caledonia.

Methods

Study site

New Caledonia is a French Territory located in the Pacific Ocean at 22°S and 165°E. Most of the studies dealing with the coral reef lagoons in this archipelago have been conducted around the city of Noumea in the southwest coast of the main island. The work presented here was conducted on the southwest lagoon of New Caledonia in an area delimited by the coast and the barrier reef between Mato pass in the south, and Uitoe pass in the north (Fig. 1). The lagoon covers an area of 2,066 km^2 (Testau and Conand 1983). Its bathymetry is very heterogeneous due to a complex geomorphology (Gabrié 1998), including shallow inner and barrier reefs, sedimentary plains, and deep canyons connected to reef passes (Fig. 1). The mean depth is 20 m, the deepest canyons reaching a depth of 60 m. The southern part of the lagoon is largely connected to the open ocean and consequently subject to significant inputs of oceanic water. Additionally, localized inputs of ocean water to the lagoon can occur through the numerous passes located along the west coast barrier reef, or over the barrier reef due to ocean swell.

The southwest lagoon is also influenced by freshwater runoff from three main rivers (Pirogues, Coulée, Dumbéa). New Caledonia is subject to tropical or subtropical meteorological conditions. River flow rates are usually low, with a yearly average value for the Dumbéa River of 5 $m^3 s^{-1}$, increasing to 300–350 $m^3 s^{-1}$ during the passage of tropical depressions of the austral summer wet season from December to April (Fig. 2). Average yearly radiation ranges from 1,000 to 2,700 Jcm^{-2}, and air temperature varies between 20 °C in August and 28 °C in February. Winds are characterized by two main directions: trade winds blowing from 60° to 160° at speeds of more than 4 ms^{-1} represent 69% of yearly wind occurrence around Noumea, corresponding to around 250 d yr^{-1}; westerly winds blowing from between 220° and 300° at speeds of more than 2 ms^{-1} represent less than 12% of yearly wind occurrence (Blaize and Lacoste 1995). This westerly wind might be of some significance, since tropical depressions and cyclones often generate winds from that direction (Fig. 3).

We mainly focused our simulation on the first river flood of January 1998 (maximum 100 $m^3 s^{-1}$), which was

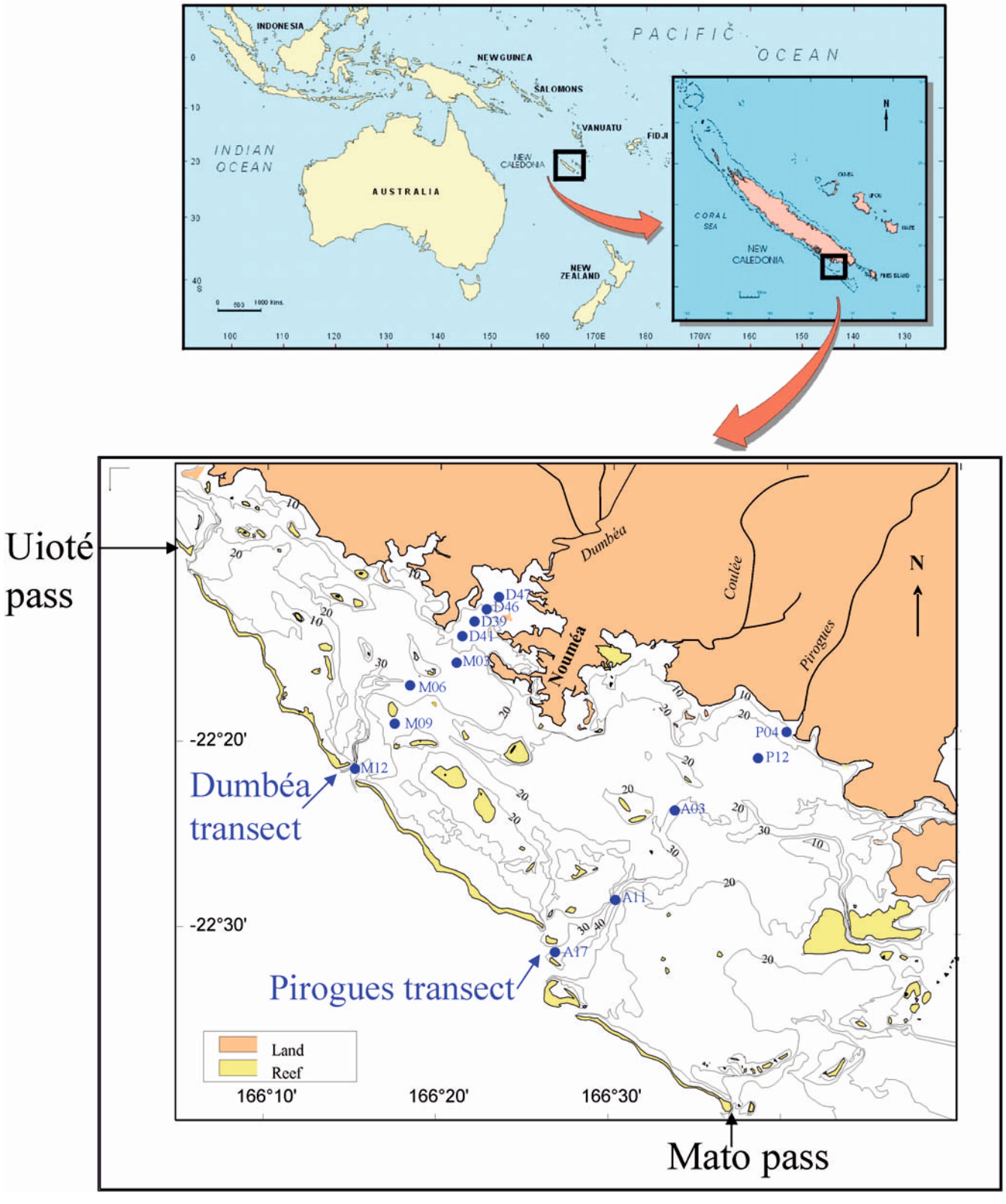

Fig. 1 Location of the New Caledonia archipelago and the southwest lagoon

slightly lower than the strongest flow in March, but occurred during stable trade wind conditions that lasted during a 1-mo period.

Hydrodynamic and physical modeling

Research on water circulation in coral reef lagoons has focused mostly on the Australian Great Barrier Reef (Frith and Mason 1986; Wolanski and King 1990;

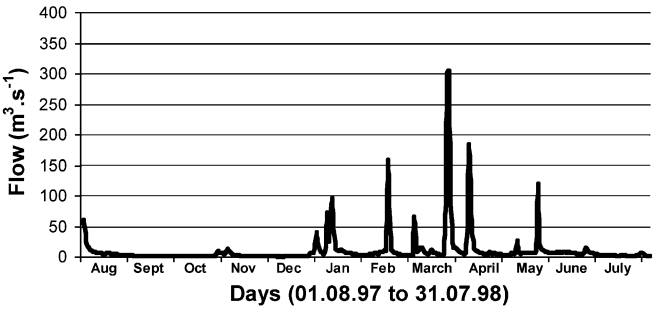

Fig. 2 Daily flow data of Dumbéa River during the period August 1997 to July 1998

Wolanski 1994; Young et al. 1994) and nuclear testing sites in the Pacific such as Enewetak (Atkinson et al. 1981), Bikini (Von Arx Ws 1948), Mururoa, and Fangataufa (Rancher 1995). Some of these studies presented two- or three-dimensional models (King 1992; Garrigues et al. 1993;Tartinville et al. 1997; Kraines et al. 1999).

Hydrodynamic studies have been conducted in New Caledonia for 25 yr (Jarrige et al. 1975; Morlière and Cremoux 1981; Morlière 1985; Rougerie 1986). More recently, an extensive hydrodynamic study was conducted with the objective of modeling water circulation in the southwest lagoon. The source code of the hydrodynamic model initially developed by IFREMER (Lazure and Salomon 1991) was adapted to the New Caledonia lagoon by Douillet (1998) and Douillet et al. (2001). In these papers, model description, circulation analysis, vertical structure of the currents, and the initial and boundary conditions were presented in detail.

The equations of the hydrodynamic model used series of classical hypotheses (e.g., Nihoul 1984; Blumberg and Mellor 1987; Ruddick et al. 1995); the Boussinesq approximation was used and the hydrostatic balance was assumed to be valid. The vertical eddy viscosity was expressed as the product of the vertical velocity gradient and of the square of the mixing length. In order to maintain a constant number of grid points on the water column, the hydrodynamic equations were solved in the σ-coordinates system (Blumberg and Mellor 1987; Hearn and Holloway 1990; Lazure and Salomon 1991; Deleersnijder and Beckers 1992). The resolution of the equations was based on the separation of the external and internal modes. To increase the model efficiency, the model equations were separated into the external and internal modes, which were simultaneously solved. The two-dimensional model calculated the elevations of the free surface (external mode) and supplied them to the three-dimensional model (internal mode); the latter fully resolved the equations. The two-dimensional model resolution was solved using the alternating direction-implicit (ADI) method (Leendertse 1967) which has been used extensively over the past 20 yr and includes automatic treatment of wetting and drying (Lazure and Salomon 1991). We used the bottom currents calculated by the three-dimensional model to compute the friction terms needed in the two-dimensional model. Spatial discretization of the equations was based on Arakawa C grid (Messinger and Arakawa 1976), slightly modified in so far as the depths and the velocity components are on the same grid point. The horizontal grid size was 500 m and each water column was divided into 21 sigma levels. This value was chosen as a compromise between the calculation capacity of the computer used and the resolution necessary to represent the geomorphologic characteristics (passes, coast, and canyons).

A complete description of the hydrodynamic circulation due to tide and to trade wind was given by Douillet et al. (2001). In our study, hydrodynamic circulation was simulated at steady-state under eight typical meteorological conditions corresponding to two wind directions (southeast for trade winds and west) and four wind speeds (4, 8, 10, and 12 m s^{-1}; Fig. 4). The hydrodynamic forcing of the biogeochemical model reproduced the time evolution of the wind measurements performed during the simulation period.

Biogeochemical modeling

Biogeochemical modeling is based on a coupled biological physical model initially developed, calibrated, and validated to simulate biogeochemical cycling in a temperate oligotrophic gulf (Pinazo et al. 1996, 2001). The biogeochemical part of the model accounts for seven state variables, which can be grouped in three different categories:

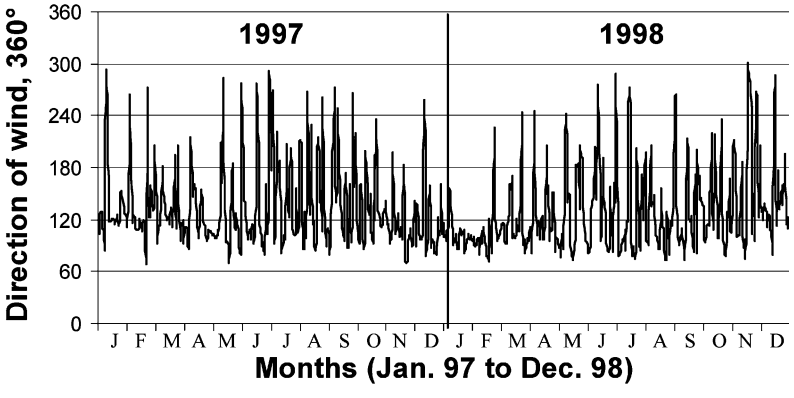

Fig. 3 Average daily direction of wind in Noumea during the period 1997–1998

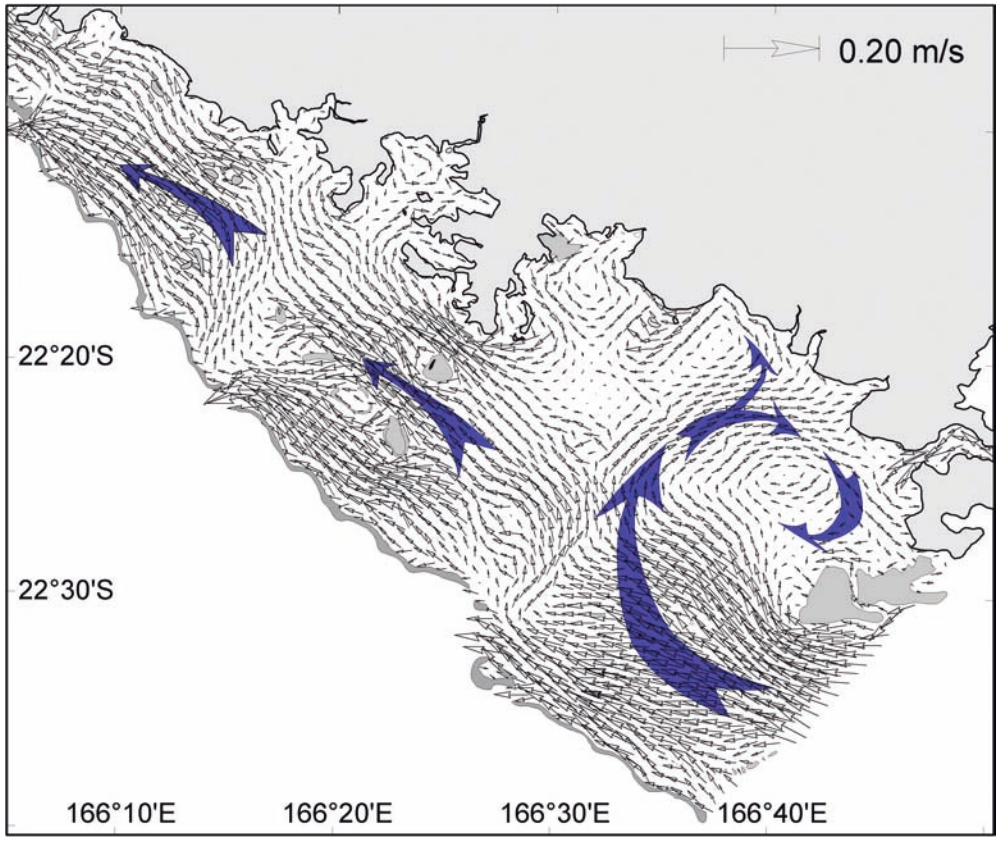

Fig. 4 Simulation of steady-state, trade-wind-induced bottom currents (trade wind of 8 m s^{-1}) from a three-dimensional hydrodynamic model (Douillet et al. 2001)

– Dissolved inorganic nutrients (nitrate, ammonium) and oxygen: (NO, NH, and O, respectively).
– Suspended organic particles with detritic carbon (C_P) and nitrogen (N_P).
– Phytoplanktonic biomass as carbon (C_B) and nitrogen (N_B)

At this first stage of fine-resolution modeling, no dissolved organic matter was considered.

Several studies suggest that silica and phosphorous do not limit phytoplankton production in such lagoons of high tropical islands (Rougerie 1986; Torreton et al. 1997). This is in agreement with Smith (1984), especially in the southwest lagoon of New Caledonia, which is characterized by a low N:P ratio of about 3:1 and a high advective throughput (residence time of 11 d; Bujan et al. 2000).

$$\frac{\partial C_B}{dt} + U\frac{\partial C_B}{\partial X} + V\frac{\partial C_B}{\partial Y} + (W + W_B)\frac{\partial C_B}{\partial Z} = \mu.(1 - \mathrm{exu}).C_B - G.C_B - \mathrm{m}.C_B - \mathrm{r}.C_B + \frac{\partial}{\partial X}\left(K_X\frac{\partial C_B}{dX}\right) + \frac{\partial}{\partial Y}\left(K_Y\frac{\partial C_B}{dY}\right) + \frac{\partial}{\partial Z}\left(K_Z\frac{\partial C_B}{dZ}\right) \quad (1)$$

The organization of the model is presented in Fig. 5. Because of the central and integrative role of phytoplankton in the model, simulation outputs of chlorophyll-*a* concentrations in the water column are mainly presented and discussed. This state variable was directly related to phytoplanktonic carbon by using an average value of 50 for the C:Chl *a* concentration ratio of coral reef lagoon phytoplankton (Charpy 1984; Garrigue 1998). The biogeochemical equations used for each state variable were presented in earlier papers (see Appendix). Only the equation for phytoplanktonic carbon biomass is presented here, the equations for other state variables being based on a similar structure.

The left hand side of the equation accounts for temporal variability, vertical and horizontal advection, and settling velocity of particles. The right hand side of the equation accounts for biogeochemical gain and loss, and turbulent diffusivities. U, V, and W were the three components of the mean velocity, respectively, in the three axes Ox, Oy, and Oz.W_B was the settling velocity of phytoplankton cells, which was equal to zero because phytoplankton cells considered in the model were very small (picophytoplankton).K_X and K_Y represented the horizontal eddy diffusivity and $K_Z$the vertical eddy diffusivity. Thus, the current velocities and the diffusivity coefficients calculated by the hydrodynamic model were used as forcing variables for the biogeochemical model. Temperature and photosynthetically available radiation (PAR) were also required to calculate biogeochemical processes.

The parameterization (Table 1) used was adapted to the tropical conditions of the southwest lagoon of New Caledonia. For phytoplankton, the parameterμ was the

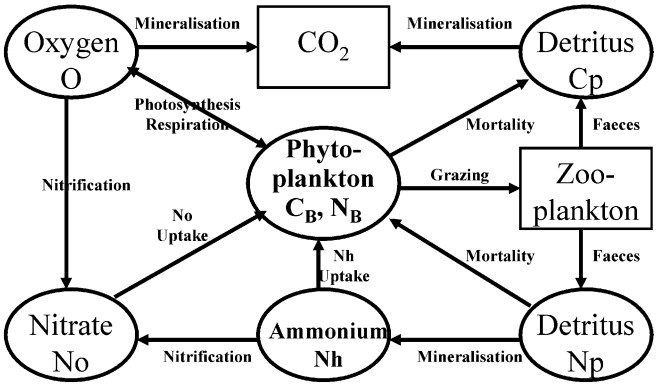

Fig. 5 Conceptual structure of biogeochemical model developed for the southwest lagoon of New Caledonia

growth rate, *EXU* was the exudation of carbon, *G* was the grazing rate, *M* was the mortality rate, and *RES* was the respiration rate.

Considering austral summer conditions, water temperature was fixed at 26.6 °C (corresponding to the mean temperature measured with a CTD in December 97 and January 98) and in situ PAR (I) data were introduced daily. Phytoplankton growth rate (μ) is dependent on temperature, light, and nutrient concentrations, the last two assumed to be limiting in New Caledonia. Growth rate (μ) was calculated according to Tett (1990) using the most restraining limiting factor:

$$\mu = \mu_{\max}.LIM \tag{2}$$

where $LIM = \min[LIM(\mathrm{I}), LIM(\mathrm{N})]$ with LIM = the limiting factor for the phytoplankton growth; $LIM(\mathrm{I})$ = the limitation by photosynthetically available radiation; and $LIM(\mathrm{N})$ = the limitation by nutrient.

$$LIM(I) = \left(\frac{I}{I_{\mathrm{opt}}}\right).e^{\left[1-\left(\frac{I}{I_{\mathrm{opt}}}\right)\right]} \tag{3}$$

where I_{opt} is the optimal photosynthetically available radiation (a higher value than I_{opt}-induced photoinhibition). $I_{\mathrm{opt}} = \frac{e}{\alpha}$ where α is the initial slope of the $LIM(I)$ curve under the threshold of photoinhibition.

$$LIM(N) = \frac{N}{K_{\mathrm{N}} + N} \text{ with } N = N_{\mathrm{B}} - (Q_0.C_{\mathrm{B}}), \tag{4}$$

where N is the concentration of nitrogen reserves of the phytoplankton cells and Q_0 is the minimum nutritional state ($N_{\mathrm{B}}/C_{\mathrm{B}}$ = cell-quota) at zero growth rate. N_{B} and C_{B} are the internal phytoplanktonic nitrogen and carbon concentrations, respectively.

In the model, we considered that 6% of the gross carbon production was lost by exudation (Bender et al. 1999). The entire assemblage of grazers modeled as a forcing variable called "zooplankton" in the biogeochemical scheme (Fig. 5). In the first step, we used constants to introduce the processes of grazing, assimilation, and excretion by zooplankton. Several studies in coral reef waters give estimates of these constants (Roman et al. 1990; Le Borgne et al. 1997; Ferrier-Pagès

Table 1 Parameters of the biogeochemical coupled model

Parameter description and symbols	Values and sources
Picophytoplankton settling velocity (W_B)	0.0 m s^{-1}
Detritus settling velocity (W_P)	10^{-5} m s^{-1}(Andersen and Nival 1988)
Maximum growth rate [$\mu_{\max}(t) = \mu_{\max 0}\ e^{b*t}$]	a = 9.851134*10^{-6} $s^{-1}$and b = 0.063321 s^{-1}(Eppley 1972)
Initial gradient of the curve LIM(I) = f(I) (alpha)	12.5*10^{-3}(J m^{-2} s^{-1})$^{-1}$(Steele 1962)
Carbon exudation of phytoplankton (exu)	6% of gross carbon production (Bender et al. 1999)
Respiration rate (RES)	5.79*10^{-6} s^{-1}(Bender et al. 1999; Langdon 1993)
Grazing rates (Gmicro and Gmeso, respectively)	1.04*10^{-5} s^{-1}microzooplankton ; 5.79*10^{-6} s^{-1}mesozooplankton (Roman et al. 1990)
Death rate (m)	0.0 s^{-1}
Maximum uptake rate for Nitrate [(upN_0)max]	4.5*10^{-6} mmol(N) [mmol(C)]$^{-1}$ s^{-1} (Caperon and Meyer 1972b)
Half-saturation constant for Nitrate (K_{N0})	0.3 mmol(N).m^{-3}(Caperon and Meyer 1972b)
Maximum uptake rate for Ammonium [(upN_H)max]	1.1*10^{-5} mmol[N) (mmol(C)]$^{-1}$ s^{-1} (Caperon and Meyer 1972b)
Half-saturation constant for Ammonium (K_{NH})	0.2 mmol(N) m^{-3}(Caperon and Meyer 1972b)
Feces fraction (f)	0.3 dimensionless (Andersen et al. 1987)
Excretion rate (e = K_e(1-f))	Ke = 0.5 dimensionless (Tett 1990)
Mineralization rate of detritic Carbon (minc)	3.47*10^{-7} s^{-1}(Peterson and Festa 1984)
Mineralization rate of detritic Nitrogen (minn)	1.042*10^{-6} s^{-1}(Andersen and Nival 1988)
Maximum nitrification rate at 0 °C [(nit_{max})0]	1.16*10^{-6} s^{-1}(Tett 1990)
Half-saturation constant for Oxygen (K_{O2})	30 mmol(O_2) m^{-3}(Tett 1990)
Attenuation coefficient of the light penetration in the water (m_2)	0.37 dimensionless (Tett 1990)
Light reflection coefficient of the sea surface (m_1)	0.95 dimensionless (Tett 1990)
Photosynthetically used radiation (m_0)	0.46 dimensionless (Tett 1990)
Minimum nutritional state at zero growth rate (Q_0)	0.05 mmol(N) [mmol(C)]$^{-1}$ (Caperon and Meyer 1972a)

and Gattuso 1998). We chose the grazing rate based on the assumption that the ecosystem of the lagoon is at equilibrium. In this case, the grazing must balance the phytoplankton net production (with a turnover time of about 1 d) minus the horizontal export rate (with a residence time of water in coastal embayments of about 10 d; Bujan et al. 2000). Thus, the grazing rate was fixed at 90% of the daily picophytoplankton net production. In the Pacific Ocean, Leborgne and Landry (personal communication) showed that a large part (up to 100%) of the production of picophytoplankton was consumed by microzooplankton.

Freshwater inputs, which induced an increase in chlorophyll-*a* concentration (more than 0.45 μg l^{-1}), unbalanced the system because (1) larger phytoplankton cells (nanophytoplankton) grow more rapidly than their grazers (mesozooplankton), and (2) the probability of a prey encountering its predator becomes lower (Torréton, personal communication). Under such freshwater input conditions, the grazing rate was fixed at 50% of the daily nanophytoplankton net production, as in the Great Barrier Reef (Roman et al. 1990).

Natural mortality of phytoplankton was ignored as trivial when compared to mortality by grazing. The parameterization used for respiration rate was based on a value of 35% of the gross primary production over 24 h (Langdon 1993; Bender et al. 1999):

$$r = 0.35.P^{B} = 0.35^{*}\mu.C_{B} \quad (5)$$

The mean value of μ was about 1.45 d^{-1}, so the respiration rate constant was taken at 0.5 d^{-1}. For the fine spatial-grid modeling of this lagoon, several tests showed a restricted influence of temperature and oxygen concentration on the variability of detritic carbon and nitrogen mineralization. Therefore, degradation of organic particles was set as an unvarying process (i.e., a constant).

Oxidation of ammonium to nitrate is mainly due to bacterial activity (Henriksen and Kemp 1988) and this process of nitrification was integrated as a function of oxygen concentration and temperature as developed in Tett and Grenz (1994). We applied a lower maximum nitrification rate in this shallow tropical lagoon than has been measured in temperate shelf areas, where the nitrification occurred mainly below the euphotic zone (Ward 2000).

Equations used to calculate nutrient consumption are similar to those previously established for the box modeling of the lagoon of New Caledonia (Bujan et al. 2000). They account for nutrient concentration in the water and the nitrogen pool in phytoplanktonic cells, which represents the nutritional state of phytoplankton related to the mean value of the nitrogen-to-carbon ratio (16:106 = 0.15) obtained by Redfield et al. (1963).

Initialization and boundary conditions (Table 2) were adjusted to field measurements and published data from the southwest lagoon (Dandonneau and Gohin 1984). Freshwater inputs from the three main rivers (Dumbéa, Coulée, Pirogues), located in the southwest part of the island (Fig. 1), were introduced in the model. Although the freshwater inputs were measured daily, the DIN supply was only measured monthly (sampled and analyzed as lagoon data). Finally, inputs from the benthos were accounted for by using measures of net benthic-pelagic nutrient fluxes (Chardy and Clavier 1988; Boucher and Clavier 1990).

Field data and simulation strategy

Sampling stations were located in the lagoon along several transects from the coast to the open sea, and around the Noumea peninsula (Fig. 1). The first transect (Dumbéa transect) followed a line from Dumbéa River to Dumbéa Pass (stations D47, D46, D9, D41, M03, M06, M09, M12; Fig. 1). The second transect located in the south part of the lagoon (Pirogues transect) followed the sample station sequence: P04, P12, A03, A11, A17 (Fig. 1).

Vertical surface to bottom profiles were conducted using a SeaBird SBE 19 CTD equipped with additional sensors for PAR (Li-Cor), turbidity (Seapoint nephelometer), and in situ chloropigment fluorometry (Wet Labs/Wet Star). Regarding data acquisition frequency versus CTD descending rate, a 25-cm resolution through the profile was obtained on average. Conversion from fluorometry to chlorophyll-*a* was obtained by correlating fluorescence data averaged between 2 and 4-m depth with discrete measurements of chlorophyll-*a* concentrations at 3 m (see below). The determination coefficient (r^2) was generally in the range 0.7–0.8.

Discrete water samples were collected using 5-L Niskin bottles and analyzed for nutrients and chlorophyll-*a*concentrations. Ammonium analysis was performed immediately after sampling according to the spectrophotometric technique initially developed by Koroleff (1976) and fully described in Aminot and Chaussepied (1983). Nitrate + nitrite (Raimbault et al. 1990) and

Table 2 Initialization conditions used for the coupled biological model

Variable	W_B[a]	W_P[b]	Chll *a*	NO_3	NH_4	O_2	Particulate carbon	Particulate nitrogen
Values	0	1.10^{-5}	0.3	0.04	0.48	180	3.3	0.5
Units	m s^{-1}	m s^{-1}	μg L^{-1}	μmol L^{-1}	μmol L^{-1}	μmol L^{-1}	μmol L^{-1}	μmol L^{-1}

[a]W_B: phytoplankton settling velocity
[b]W_P: detritus settling velocity

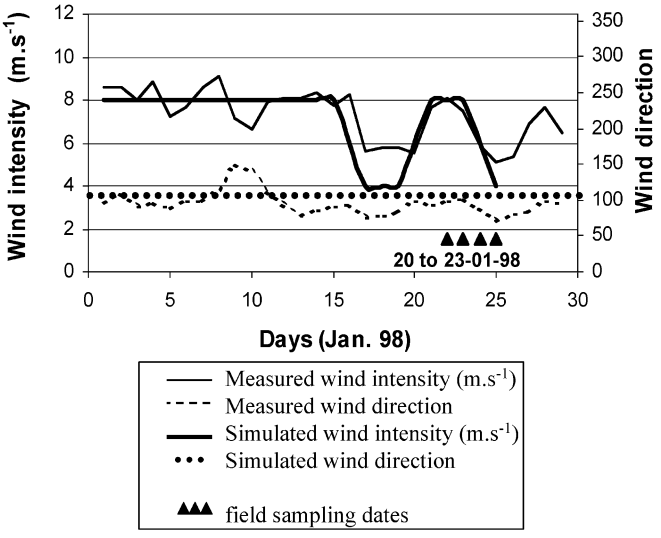

Fig. 6 Comparison between field measurements and simulated wind conditions used for the realistic scenario in January 1998. Locations of the stations are given in Fig. 1

phosphate (Murphy and Riley 1962) were analyzed according to automated colorimetric procedures using a Techicon Autoanalyser II after storage of the samples in a deep freeze. Chlorophyll-*a* concentrations were determined by fluorimetry (Yentsch and Menzel 1963) on a Turner Design 700 fluorimeter after filtration on GF/F Watman glass-fiber filters (pore size 0.7 μm).

We used a succession of different forcing to reproduce wind field measurements during the year 1998. The entire simulation corresponds to the biogeochemical response of the southern lagoon segment to the meteorological conditions measured in January 1998 (Fig. 6). This period was representative of the beginning of the summer wet-season, with relatively constant trade wind conditions. The first 2 wk were dominated by a sustained trade wind of 8 ms^{-1}, followed by a succession of different trade wind velocities: 3 d at 4 m s^{-1}, 3 d at 8 m s^{-1} (Fig. 4), and a last day at 4 m s^{-1}.

Results

Vertical chlorophyll-*a* distribution derived from fluorometry profiles (Fig. 7) demonstrated vertical homogeneity in the top 10 m of the water column and validated model outputs. Considering this homogeneity, the 3-m depth level of the three-dimensional model was considered as representative of the concentration in the lagoon surface waters and was used for comparison with in situ data from water collected at 3 m.

Except for ammonium, model outputs after a simulated period of 3 wk were strongly correlated with observed data (Fig. 8). Correlation coefficients were significant for particulate organic nitrogen (PON) ($r = 0.72$**) and highly significant for chlorophyll-*a* ($r = 0.88$***) and particulate organic carbon (POC) ($r = 0.75$***) with a probability $\alpha < 0.01$ ($n = 16$)

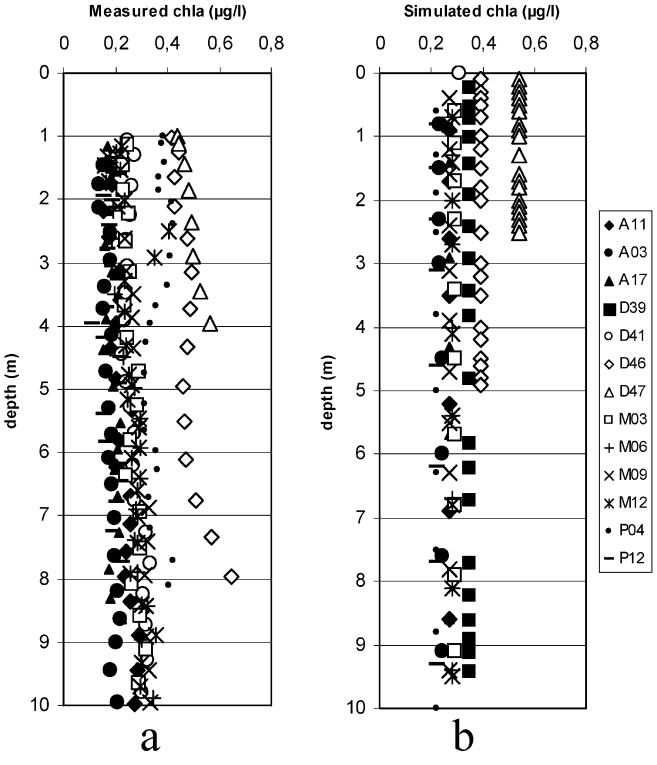

Fig. 7 Vertical profiles of chlorophyll-*a* (**a**) calculated from CTD fluorescence data in the southwest lagoon of New Caledonia in January 1998, and (**b**) simulated after 22 simulation days (expressed in μg l^{-1})

Focusing on chlorophyll-*a*, we observed that model outputs mirrored the actual distribution of concentrations across the lagoon, with a strong decreasing gradient from coast to middle lagoon, followed by a slight increase toward the back reef (Fig. 9). Samples from January 1998 confirmed a general trend showing that middle lagoon waters were slightly more enriched in the northern part of the lagoon than in the southern part, where water residence time is shorter (Fichez et al., unpublished data).

For a more detailed comparison, results from three stations that could be considered as representative of specific lagoon conditions were selected. Station D47, the nearest to the Dumbéa River estuary, represented coastal environments directly influenced by river inflows. Station M03, located a few km from D47 in front of the Dumbéa Bay, represented middle lagoon conditions potentially influenced by significant run-off events. Station A03 presented typical middle lagoon conditions in the southern part of the lagoon with minimal nutrient and chlorophyll-*a* levels. At those three stations, initial nutrient concentrations were rapidly balanced by terrigenous nutrient supply. After 22 d of realistic simulation corresponding to January 1998, the molar nitrogen/carbon ratio was 0.23, higher than the Redfield molar nitrogen/carbon ratio of 0.15. This ratio corresponded to well-nourished phytoplankton cells with maximum growth rate stabilized at a value of 4.10^{-5} s^{-1}(slightly less

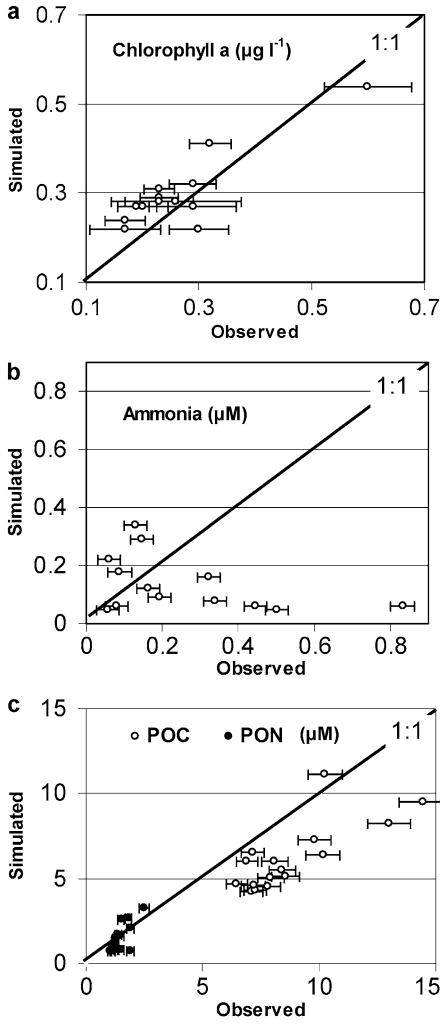

Fig. 8 Simulated versus observed data: (**a**) chlorophyll-*a* concentrations with error bars corresponding to uncertainties calculated from the vertical variation of fluorescence data between 2- and 4-m depth (range between 2 and 12%); (**b**) ammonium concentrations with a precision of 30 nM (Diaz and Raimbault 2000); and (**c**) particulate organic carbon and nitrogen concentrations in µmol/l with a precision of 7 and 8.5%, respectively (Raimbault et al. 1999)

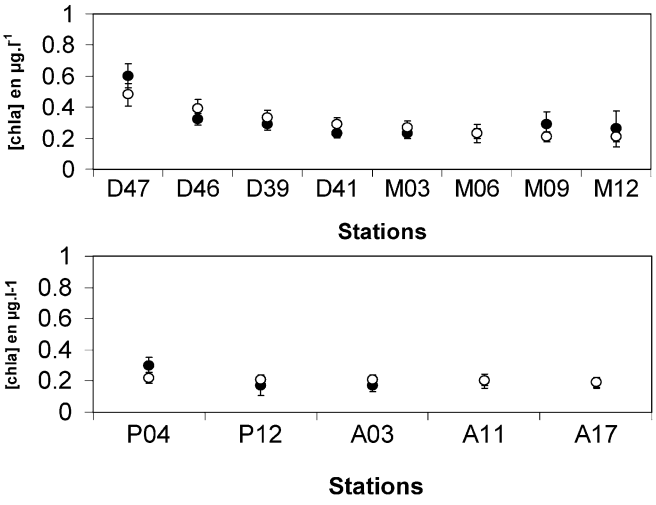

Fig. 9 Field data (*closed circles*) and simulated (*open circles*) surface chlorophyll-*a* concentration (expressed in µg/L) in January 1998: (**a**) at eight stations located along the coast to ocean "Dumbéa" transect, and (**b**) at five stations located along the coast to ocean "Pirogues" transect. Error bars for simulated chlorophyll-*a* correspond to the maximum variation (15% for an increase of 10% of the maximum growth rate) calculated in sensitivity analysis. Error bars for measured chlorophyll-*a* correspond to uncertainties calculated from the vertical variation of fluorescence data between 2- and 4-m depth (range between 2 and 12%)

than two divisions per day). This result suggests that phytoplankton requirements for nitrogen were met by terrestrial nutrient inputs. At station D47, chlorophyll-*a*concentrations exceeding 0.5 µg L^{-1} would be a consequence of river inputs and associated development of nanophytoplankton communities less sensitive to mesozooplankton grazing. At station M03, outside Dumbéa Bay, trade winds were responsible for nutrient and phytoplankton export to the north, sustaining chlorophyll-*a*concentrations of about 0.3 µg L^{-1}. At station A03, located in the central part of the south lagoon, the increased influence of hydrodynamic inputs of oceanic waters from the south slightly lowered chlorophyll-*a* concentrations below 0.25 µg L^{-1}.

The spatial patterns of the main state variables (ammonium and chlorophyll-*a*, respectively) for this January 1998 scenario are shown in Figs. 10 and 11. Simulated distribution of ammonium showed the river plume in Dumbéa Bay to extend along the north coast (Fig. 10). Terrigenous inputs from the Coulée and Pirogues Rivers in the south did not result in significant plumes because oceanic water inputs coming from the open southern boundary of the lagoon almost immediately diluted these river inputs. Maximum river flow occurred after 10 d of simulation in January 1998, increasing to 100 m^3 s^{-1} for the Dumbéa River (Fig. 2). The simulated pattern of ammonium concentrations portrayed the generally oligotrophic character of this pelagic system, except in the Dumbéa Bay and near the northern coast where river inputs, higher residence time, and long-shore transport favored higher nutrient levels.

Simulated distribution of phytoplankton (expressed in chlorophyll-*a* concentrations) at 3-m depth after 22 d of this summer scenario are given in Fig. 11. The trade wind influence rapidly increased in time and extended from the south over a large part of the lagoon, inducing low chlorophyll-*a* concentrations in most of the lagoon (less than 0.3 µg L^{-1}). Phytoplankton-poor oceanic waters entered the lagoon from the south and the Woodin channel, and rapidly extended northward (11 d; Bujan et al. 2000). Highest values of chlorophyll-*a* were observed in and close to the most enclosed bays, Dumbéa Bay appearing to be the most enriched system under natural conditions. Due to their geomorphological features, these bays are partly sheltered from trade winds, favoring longer water residence time and the subsequent build-up of phytoplankton biomass. Additional freshwater inputs in

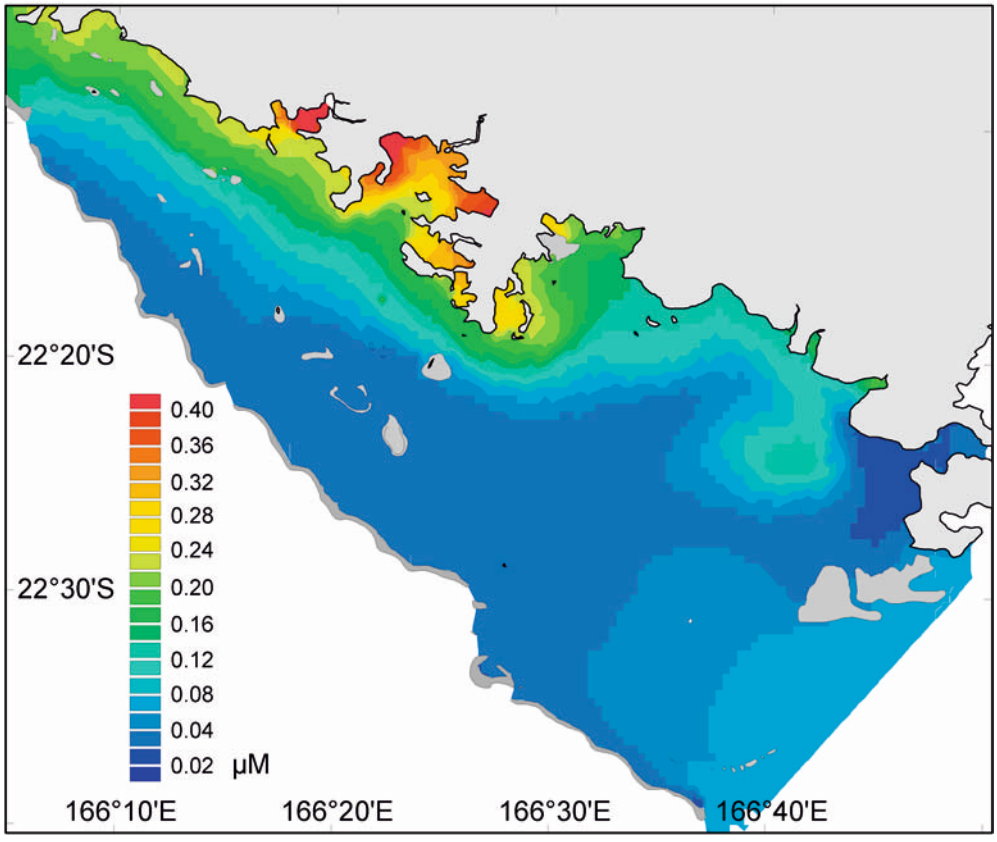

Fig. 10 Pattern of ammonium concentration at 3-m depth after 22 simulation days, using realistic scenario in January 1998

Dumbéa Bay resulted in a simulated phytoplankton growth of 0.48 µg L^{-1} (Fig. 11). Although this simulation showed a slight heterogeneity in chlorophyll-*a*concentrations, the whole lagoon exhibited a low biomass at any time, especially in the southwestern part of the lagoon, just behind the barrier reef and above the white sand sediments (Chardy et al. 1988). Outputs of lagoonal waters were observed through the passes as shown by the existence of plumes of slightly higher chlorophyll-*a* concentration entering the Coral Sea where oligotrophic conditions with very low chlorophyll-*a* concentrations (about 0.05 µg L^{-1}) prevailed.

Sensitivity analysis of parameters

A sensitivity analysis of the model parameters was performed using the sensitivity index presented by Chapelle et al. (2000). Each parameter was modified by ±10% and the results of each run were analyzed using the IS% index:

$$IS\% = \left(\frac{100}{p}\right) * \frac{1}{n}\sum_{i=1}^{n}\frac{\left|X_i - X_i^{\mathrm{ref}}\right|}{X_i^{\mathrm{ref}}} \qquad (6)$$

where p is the % of the parameter variation (±10%),X_{i} is the new variable value, and X_i^{ref} is the January 1998 reference variable-value. Dividing by p in the IS% equation leads to the % variation of each modeled variable per % variation of each parameter. The result was averaged over n, which corresponds to the number of grid points (2,039) multiplied by the 25 d of simulation ($n = 50975$).

The sensitivity results for the four state variables, chlorophyll-*a*, phytoplankton nitrogen, ammonia, and nitrate concentrations, are given in Fig. 12. Results for the other state variables are not presented because their variations were lower than 0.1%, whatever the parameter considered.

Even though phytoplankton (expressed in chlorophyll-*a* or nitrogen content) and DIN (ammonium and nitrate concentrations) were the most sensitive variables in the model, a maximum variation of 1.5% was measured for chlorophyll-*a* concentrations. Results from this model output sensitivity analysis were used to calculate the simulated variable errors as plotted for chlorophyll-*a* concentrations in Fig. 9. This numerical variability was in the same order of magnitude as the measured variability in the field data.

Only four (phytoplankton growth, respiration, light limitation, and microzooplankton) grazing parameters and five (phytoplankton growth, respiration, microzooplankton grazing, nitrogen mineralization, and nitrification parameters) parameters modified phytoplankton biomass and DIN standing stock, respectively, by more than 0.1%.

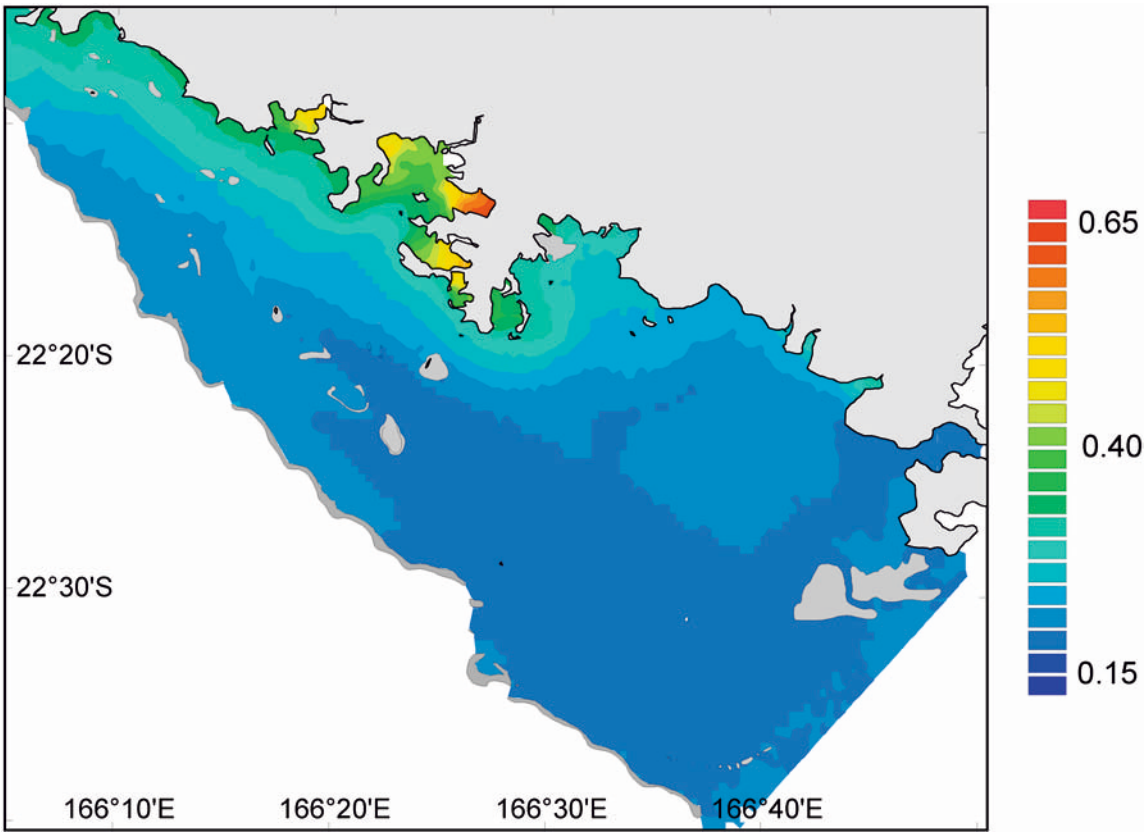

Fig. 11 Pattern of chlorophyll-a concentration at 3-m depth after 22 simulation days, using realistic scenario in January 1998

Discussion

The homogeneous vertical distribution of chloropigments in the 10-m-top layer generated by the model was confirmed by in situ data (Fig. 7), as typically observed in coastal tropical areas (Sorokin 1993). Moreover, comparison between simulation and field data in January 1998 showed a significant correlation between modeled and measured data, except for ammonium (Fig. 8), where the low measured and simulated concentrations were not significantly correlated. The slight discrepancy between measured and modeled POC concentrations (Fig. 8c) could be explained by the fact that the source of particulate organic carbon, derived from both land and reef, and maximal during the summer (Clavier et al. 1995), was not taken into account in the model. The most distant points from the 1:1 line corresponded to stations located close to the shore or to the barrier reef.

Measured chlorophyll-*a* concentrations were slightly lower than model outputs in the central part of the lagoon (Figs. 9 and 11). This could be explained by an underestimation of the extension of the oligotrophic plume originating from the south boundary under trade wind conditions. The classification of wind conditions in fixed intervals used to run the model is a source of uncertainties. From January 17 to 19, recorded wind speeds of 6 m s^{-1} were converted to a simulated average wind speed of 4 m s^{-1} (Fig. 6). Improving the wind forcing parameterization by using full physical versus biological coupling would be required to better describe the oligotrophic plume extension and compensate for the slight gap between simulated and observed chlorophyll-*a*concentrations in the central part of the lagoon.

The sensitivity analysis of the coupled physical-biogeochemical model (Fig. 12) showed that this model is weakly sensitive to the biogeochemical parameter values, and that the simulation results are mainly influenced by the physical forcing and subsequent water transport process. The maximum variation observed on modeled chlorophyll-*a* concentrations in the sensitivity analysis were in the same order of magnitude as the standard deviation of the measured chlorophyll-*a*concentrations (15% or less).

The simulation presented in this study aims at assessing the large-scale distribution of chlorophyll-*a* concentrations as a function of different hydrodynamic conditions and freshwater inputs. No limitation by nutrients was detected at stations at the mouth of the Dumbéa and Pirogues Rivers subject to significant freshwater inputs. The hydrodynamic influence on phytoplankton dynamics was reduced because of the relative stability of the waters in Dumbéa Bay, sheltered by the Noumea peninsula. Conversely, simulation results for the Pirogues River mouth showed a very strong hydrodynamic influence that rapidly dispersed river-

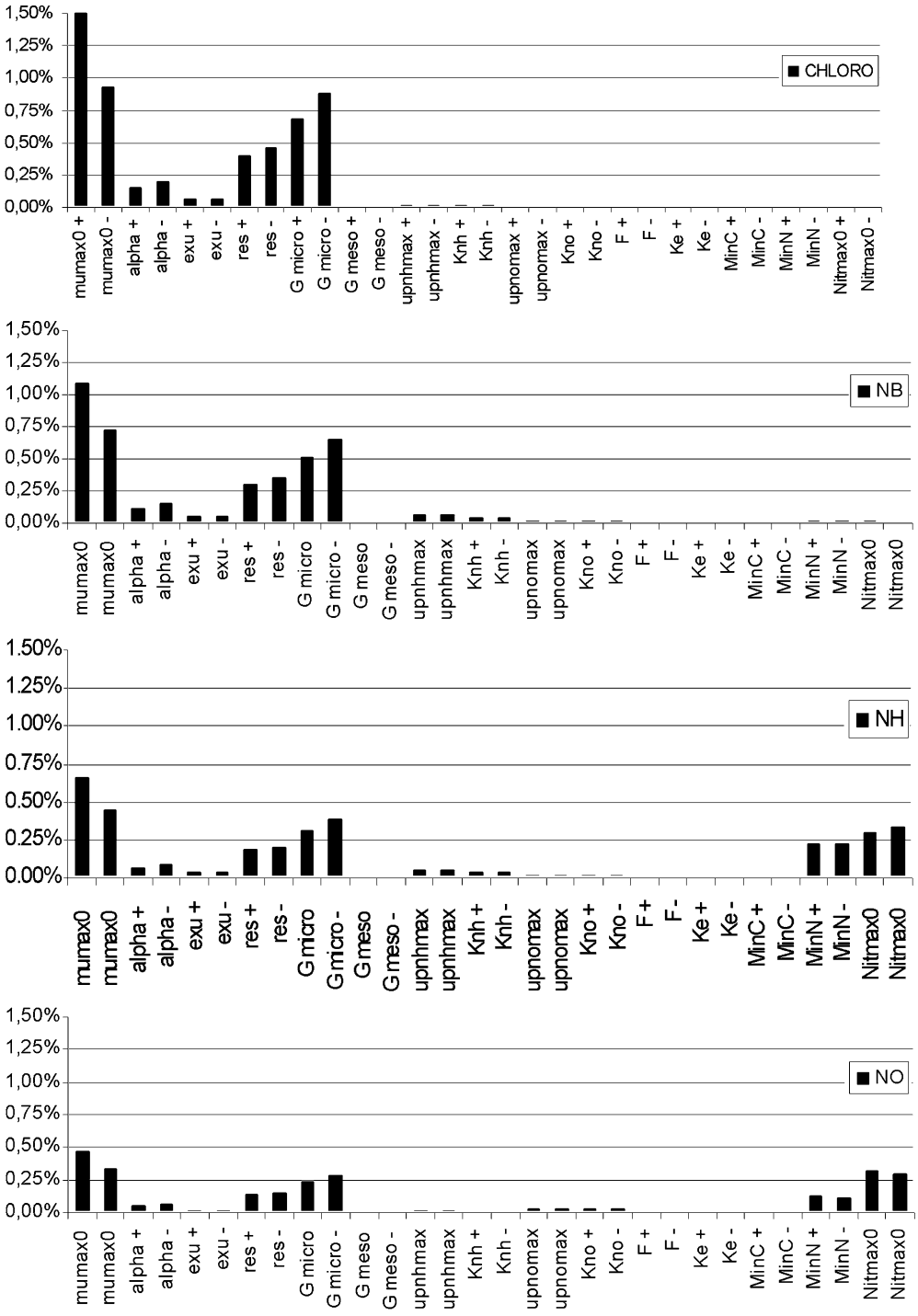

Fig. 12 Average IS% index (considering all grid points and time steps) calculated in the sensitivity analysis for the four most sensitive state variables: phytoplankton biomass expressed in chlorophyll-*a* (Chl *a*) and nitrogen concentrations (*NB*), and DIN expressed in ammonium (*NH*) and nitrate (*NO*) concentrations (see Table 2 for parameter description)

borne nutrient inputs and subsequent phytoplankton biomass.

Further offshore, differences in phytoplankton dynamics were more pronounced. Nitrogen limitation of phytoplankton growth was predicted a few kilometers from Dumbéa River and in front of the Dumbéa Bay (station M03; Figs. 9a 11). Phytoplankton concentration was logically lower at M03 than at station D47, as a consequence of greater increased hydrodynamically driven dilution.

Central locations in the southern part of the lagoon, (e.g., station A03 Figs. 9b and 11) showed the strong influence of oceanic inputs. The inflow of oligotrophic waters renewed lagoon waters in a matter of days to weeks, maintaining low phytoplankton concentrations. Moreover, an increase in wind forcing resulted in an increase in water replacement that further reduced simulated nutrient and chlorophyll-*a*concentrations down to near-ultra-oligotrophic ocean conditions. Desrosieres (1975) previously observed a similar pattern.

In parallel to low phytoplankton biomass, the model predicts a high growth rate maintained in the initial oceanic water conditions. This result shows that during favorable hydrodynamic conditions at station A03 (low or westerly wind) combined with sustained freshwater inputs, phytoplankton biomass should increase slightly before being limited by nutrient availability.

The results of the simulation after 3 wk (Fig. 11) under a combination of several realistic forcing scenarios emphasized a generally decreasing phytoplankton concentration gradient from the coast to the open sea, with highest values around Noumea peninsula. The results of the simulations were in good agreement with field observations, providing a first validation of our model of this tropical pelagic coastal ecosystem. Considering the relative complexity of the simulations due to the use of a fine spatial grid, we were able to differentiate among the main abiotic forcings.

Except for coastal areas located near the river mouths, the influence of oceanic waters constitutes the main factor that drives chlorophyll-*a* concentrations in the lagoon. Strong advection and turbulent diffusion of oceanic waters (Fig. 4) combined with low values of nitrogen maintained a minimum concentration of phytoplankton inside the lagoon, which increased as soon as nutrients became more available. For instance, the nitrate inputs due to river flooding events during the summer wet season generated an increase in phytoplankton biomass corresponding to the growth of large phytoplankton species, which were taken into account in our model by a lower grazing rate by mesozooplankton than by microzooplankton. The impact of the recorded freshwater input events on the lagoon as a whole was limited to a simulated chlorophyll-*a* increase of 0.48 μg L^{-1} (to be compared with the measured chlorophyll-*a* increase of 0.6 μg L−1) that could not be truly labeled as a phytoplankton bloom. At any time in the entire Caledonian lagoon, maximum measured chlorophyll-*a* concentrations rarely exceeded 1.2 μg L^{-1} (Rougerie 1986; Fichez et al., unpublished data).

Eight categories of wind velocity range chosen as representative of the most common recorded wind conditions were used to limit calculation time. Hydrodynamic and biogeochemical models were developed separately (offline) to enable affordable simulation runs. Unfortunately, the offline use of the models underestimated realistic trade wind forcing and thus the extension of the oligotrophic waters into the lagoon. A further improvement of our work will be to run the hydrodynamic and biogeochemical models on-line.

At this stage of development, the physical model did not account for swell-generated, cross-reef hydrodynamics, which are known to be a very complex issue in tidal systems (Hata et al. 1998). Hydrodynamic modeling in the lagoon coupled with extensive current profiling demonstrated that even if swell-generated, cross-reef currents might have a local impact on water circulation in the back reef area, the semi-diurnal tide and, more importantly, wind-induced advection were the two main factors driving water currents in this part of the New Caledonia lagoon (Douillet 1998). Modeling waves in the lagoon might be a much more significant issue because of the major impact of waves on particle resuspension and subsequent particle transport in shallow coastal areas (Douillet et al. 2001).

The box model approach used in a previous study (Bujan et al. 2000) showed that the freshwater influence was limited to the coastal boxes and that the typical lagoon areas presented oligotrophic characteristics. The use of the three-dimensional model provides a more precise description of the variability in phytoplankton spatial distributions related to nutrient inputs. For instance, in the box model, the Dumbéa Bay area was represented by just two boxes, while the three-dimensional model results clearly showed strong gradients in this bay as a function of wind forcing. The same comments apply to the passes near the reef boundaries where the box model poorly reflected the biogeochemical impact of complex circulation processes. The three-dimensional model results will be used to define sampling strategies for further fieldwork in the southwest lagoon.

Simulation outputs supported by in situ data demonstrated that the lagoon could be divided into (1) sheltered bays experiencing freshwater inputs and restricted exchanges with the open lagoon, (2) nearshore regions influenced occasionally by river discharges, with lower water residence times, and (3) central parts of the lagoon, not significantly influenced by rivers, but strongly controlled by the flushing of oceanic waters mainly entering from the southeastern boundary (trade winds conditions). Despite localized areas of enhanced productivity in sheltered coastal bays, the lagoon as a whole can be classified as an oligotrophic system when compared to continental coastal zones. Standard simulation considering an extreme scenario with a tenfold increase in nitrogen concentration in the rivers resulted in a low increase in phytoplankton biomass, with a maximum chlorophyll-*a* concentration of 1.69 μg L^{-1} in Dumbéa Bay. This three-dimensional simulation was consistent with the previous long-term box model simulation (Bujan et al. 2000) and confirmed the resilience of the oligotrophic status of the lagoon.

Future improvement of the modeling approach would include on-line coupling of hydrodynamic and biogeochemical models, and a more detailed and adapted mathematical description of the pelagic system, including phytoplankton physiology (growth, respiration, light limitation), microzooplankton grazing, and nitrogen regeneration due to the microbial loop.

Acknowledgements We thank all the IRD Ecotrope staff for fieldwork and analysis, the Centre Meteo-France in Noumea for providing meteorological data, and the specialists of zooplankton, phytoplankton, and microplankton of the IRD Center of Noumea. This work was supported by IRD and the PNEC (Programme National Environnement Côtier).

Appendix 1: Equations of the biogeochemical coupled model.

– Phytoplankton biomass expressed in carbon:

$$\underbrace{\frac{\partial C_B}{\partial t}+u\frac{\partial C_B}{\partial x}+v\frac{\partial C_B}{\partial y}+}_{\text{advection}}\ \underbrace{(w+w_B)\ \left(\frac{\partial C_B}{\partial z}\right)}_{\text{sink}}=\underbrace{\mu\cdot(1-\text{exu})\cdot C_B}_{\text{growth}}-\underbrace{G\cdot C_B}_{\text{grazing}}-\underbrace{m\cdot C_B}_{\text{death}}-\underbrace{r\cdot C_B}_{\text{respiration}}+\underbrace{\frac{\partial}{\partial x}\left(K_x\frac{\partial C_B}{\partial x}\right)+\frac{\partial}{\partial y}\left(K_y\frac{\partial C_B}{\partial y}\right)+\frac{\partial}{\partial z}\left(K_z\frac{\partial C_B}{\partial z}\right)}_{\text{diffusion}} \tag{7}$$

– Phytoplankton biomass expressed in nitrogen:

$$\underbrace{\frac{\partial N_B}{\partial t}+u\frac{\partial N_B}{\partial x}+v\frac{\partial N_B}{\partial y}+}_{\text{advection}}\ \underbrace{(w+w_B)\left(\frac{\partial N_B}{\partial z}\right)}_{\text{sink}}=\underbrace{up\cdot C_B}_{\text{uptake}}-\underbrace{G\cdot N_B}_{\text{grazing}}-\underbrace{m\cdot N_B}_{\text{death}}+\underbrace{\frac{\partial}{\partial x}\left(K_x\frac{\partial N_B}{\partial x}\right)+\frac{\partial}{\partial y}\left(K_y\frac{\partial N_B}{\partial y}\right)+\frac{\partial}{\partial z}\left(K_z\frac{\partial N_B}{\partial z}\right)}_{\text{diffusion}} \tag{8}$$

– Particulate detritic carbon:

$$\underbrace{\frac{\partial C_P}{\partial t}+u\frac{\partial C_P}{\partial x}+v\frac{\partial C_P}{\partial y}+}_{\text{advection}}\ \underbrace{(w+w_P)\left(\frac{\partial C_P}{\partial z}\right)}_{\text{sink}}=\underbrace{f\cdot G\cdot C_B}_{\text{feces}}+\underbrace{m\cdot C_B}_{\text{death}}-\underbrace{\min c\cdot C_P}_{\text{mineralization}}+\underbrace{\frac{\partial}{\partial x}\left(K_x\frac{\partial C_P}{\partial x}\right)+\frac{\partial}{\partial y}\left(K_y\frac{\partial C_P}{\partial y}\right)+\frac{\partial}{\partial z}\left(K_z\frac{\partial C_P}{\partial z}\right)}_{\text{diffusion}} \tag{9}$$

– Particulate detritic nitrogen:

$$\underbrace{\frac{\partial N_P}{\partial t}+u\frac{\partial N_P}{\partial x}+v\frac{\partial N_P}{\partial y}+}_{\text{advection}}\ \underbrace{(w+w_P)\left(\frac{\partial N_P}{\partial z}\right)}_{\text{sink}}=\underbrace{f\cdot G\cdot N_B}_{\text{feces}}+\underbrace{m\cdot N_B}_{\text{death}}-\underbrace{\min n\cdot N_P}_{\text{mineralization}}+\underbrace{\frac{\partial}{\partial x}\left(K_x\frac{\partial N_P}{\partial x}\right)+\frac{\partial}{\partial y}\left(K_y\frac{\partial N_P}{\partial y}\right)+\frac{\partial}{\partial z}\left(K_z\frac{\partial N_P}{\partial z}\right)}_{\text{diffusion}} \tag{10}$$

– Dissolved ammonia:

$$\underbrace{\frac{\partial N_H}{\partial t}+u\frac{\partial N_H}{\partial x}+v\frac{\partial N_H}{\partial y}+w\left(\frac{\partial N_H}{\partial z}\right)}_{\text{advection}}=\underbrace{-upN_H\cdot C_B}_{\text{uptake}}+\underbrace{e\cdot G\cdot N_B}_{\text{excretion}}+\underbrace{\min n\cdot N_P}_{\text{mineralization}}-\underbrace{nit\cdot N_H}_{\text{nitrification}}+\underbrace{\frac{\partial}{\partial x}\left(K_x\frac{\partial N_H}{\partial x}\right)+\frac{\partial}{\partial y}\left(K_y\frac{\partial N_H}{\partial y}\right)+\frac{\partial}{\partial z}\left(K_z\frac{\partial N_H}{\partial z}\right)}_{\text{diffusion}} \tag{11}$$

– Dissolved nitrate:

$$\underbrace{\frac{\partial N_o}{\partial t}+u\frac{\partial N_o}{\partial x}+v\frac{\partial N_o}{\partial y}+w\left(\frac{\partial N_o}{\partial z}\right)=}_{\text{advection}}\ \underbrace{-upN_o\cdot C_B}_{\text{uptake}}+\underbrace{nit\cdot N_H}_{\text{nitrification}}+\underbrace{\frac{\partial}{\partial x}\left(K_x\frac{\partial N_o}{\partial x}\right)+\frac{\partial}{\partial y}\left(K_y\frac{\partial N_o}{\partial y}\right)+\frac{\partial}{\partial z}\left(K_z\frac{\partial N_o}{\partial z}\right)}_{\text{diffusion}} \tag{12}$$

– Dissolved oxygen:

$$\underbrace{\frac{\partial O}{\partial t}+u\frac{\partial O}{\partial x}+v\frac{\partial O}{\partial y}+w\frac{\partial O}{\partial z}=}_{\text{advection}}\ \underbrace{\mu\cdot C_B}_{\text{growth}}-\underbrace{r\cdot C_B}_{\text{respiration}}-\underbrace{\min c\cdot C_P}_{\text{mineralization}}-\underbrace{2nit\cdot N_H}_{\text{nitrification}}+\underbrace{2upN_o\cdot C_B}_{\text{reduction}}+\underbrace{\frac{\partial}{\partial x}\left(K_x\frac{\partial O}{\partial x}\right)+\frac{\partial}{\partial y}\left(K_y\frac{\partial O}{\partial y}\right)+\frac{\partial}{\partial z}\left(K_z\frac{\partial C_B}{\partial z}\right)}_{\text{diffusion}} \tag{13}$$

References

Aksnes DG, Ulvestad KB, Baliño BM, Berntsen J, Egge JK, Svendsen E (1995) Ecological modelling in coastal waters: towards predictive physical-chemical-biological simulation models. Ophelia 41:5–36

Aminot A, Chaussepied M (1983) Manuel des analyses chimiques en milieu marin. CNEXO, Brest, France, pp 107–118

Andersen V, Nival P, Harris P (1987) Modelling of a planktonic ecosystem in an enclosed water column. J Mar Biol Assoc UK 67:407–430

Andersen V, Nival P (1988) A pelagic ecosystem model simulating production and sedimentation of biogenic particles: role of slaps and copepods. Mar Ecol Prog Ser 44:37–50

Arias-Gonzales E (1993) Fonctionnement trophique d'un écosystème récifal: secteur de Tiahura, île de Moorea, Polynésie Française. Thèse de Doctorat, Université de Perpignan, 250 pp

Atkinson MJ, Grigg W (1984) Model of a coral reef ecosystem II: gross and net benthic primary production at French Frigate Shoals, Hawaii. Coral Reefs 3:13–22

Atkinson MJ, Smith SV, Stroup (eds) (1981) Circulation in Enewetak atoll lagoon. Limnol Oceanogr 26:1074–1083

Bender M, Orchardo J, Dickson ML, Barber R, Lindley S (1999) In vitro O_2 fluxes compared with 14C production and other rate terms during the JGOFS Equatorial Pacific experiment. Deep Sea Res I 46:637–654

Billen G (1978) A budget of nitrogen recycling in North Sea sediments of the Belgian coast. Estuar Coast Mar Sci 7:127–146

Billen G, Lancelot C (1988) Modelling benthic nitrogen cycling in temperate coastal ecosystems. In: Blackburn TH, Sørensen J (eds) Nitrogen cycling in coastal marine environments. Wiley, New York, pp 341–378

Blaize S, Lacoste D (1995) Atlas climatique de la Nouvelle Calédonie. Météo-France, Nouméa, Nouvelle-Calédonie, 104 pp

Blumber AF, Mellor GL (1987) A description of the three-dimensional coastal ocean circulation model. In: Heaps N S (ed) Three-dimensional coastal ocean model: American Geophysical Union, Washington DC, pp 1–16

Boucher G, Clavier J (1990) Contribution of benthic biomass to overall metabolism in New Caledonia lagoon sediments. Mar Ecol Prog Ser 64:271–280

Bujan S (2000) Modelisation biogeochimique du cycle du Carbone et de l Azote dans les écosystèmes côtiers tropicaux sous influences terrigène et anthropique: Application au lagon de Noumea (Nouvelle Calédonie). PhD Thesis University of Mediterranee, Aix-Marseille, 205 pp

Bujan S, Grenz C, Fichez R, Douillet P (2000) Biogeochemical recycling in south-west lagoon of New Caledonia: box model approach. C R Acad Sci 323:225–233

Caperon J, Meyer J (1972a) Nitrogen-limited growth of marine phytoplankton. I Changes in population characteristics with steady-state growth rate. Deep Sea Res 19(A):601–618

Caperon J, Meyer J (1972b) Nitrogen-limited growth of marine phytoplankton. II Uptake kinetics and their role in nutrient-limited growth of phytoplankton. Deep Sea Res 19(A):619–632

Chapelle A, Menesguen A, Deslou-Paoli J-M, Souchu P, Mazouni N, Vaquer A, Millet B (2000) Modelling nitrogen, primary production and oxygen in a Mediterranean lagoon: impact of oysters farming and inputs from the watershed. Ecol Model 127:161–181

Chardy P, Clavier J (1988) Biomass and trophic structure of the macrobenthos in the south-west lagoon of New Caledonia. Mar Biol 99:195–202

Chardy P, Chevillon C, Clavier J (1988) Major benthic communities of the south-west lagoon of New Caledonia. Coral Reefs 7:69–75

Charpy L (1984) Quelques caractéristiques de la matière organique particulaire du lagon. L'atoll de Tikehau. Notes et documents d'océanographie n 22. ORSTOM Polynésie Française

Christensen V, Pauly D (1992) ECOPATH II-a software for balancing steady-state ecosystems models and calculating network characteristics. Ecol Model 61:169–185

Clavier J, Chardy P, Chevillon C (1995) Sedimentation of particulate matter in the South-west lagoon of New Caledonia: spatial and temporal patterns. Estuar Coast Shelf Sci 40:281–294

Dandonneau Y, Gohin F (1984) Meridional and seasonal variations of the sea surface chlorophyll concentration in the south-western tropical pacific (14 to 32°S, 160 to 175°E). Deep Sea Res 31(12):1377–1393

Deleersnijder E, Beckers JM (1992) On the use of the σ-coordinate system in regions of large bathymetric variations. J Mar Syst 3:381–390

Desrosieres R (1975) Quelques observations sur le phytoplancton océanique des abords de la Nouvelle-Calédonie (océan Pacifique sud-ouest). Norw J Bot 22:195–200

Diaz F, Raimbault P (2000) Nitrogen regeneration and dissolved organic nitrogen release during spring in a NW Mediterranean coastal zone (Gulf of Lions): implications for the estimation of new production. Mar Ecol Prog Ser 197:51–65

Douillet P (1998) Tidal dynamics of the south-west lagoon of New Caledonia: observations and 2D numerical modelling. Oceanol Acta 21(1):69–79

Douillet P, Ouillon S, Cordier E (2001) A numerical model for fine suspended sediment transport in the south-west lagoon of New Caledonia. Coral Reefs 20:361–372

Eppley RW (1972) Temperature and phytoplankton growth in the sea. Fish Bull 70:1063–1085

Fasham MJR, Ducklow HW, Mickelie SM (1990) A nitrogen-based model of plankton dynamics in the ocean mixed layer. J Mar Res 48:591–639

Ferrier-Pagès C, Gattuso J-P (1998) Biomass, production and grazing rates of pico and nanoplankton in coral reef waters (Miyako Island, Japan). Microb Ecol 35:46–57

Frith CA, Mason LB (1986) Modelling wind driven circulation, One Tree Reef, Southern Great Barrier Reef. Coral Reefs 4:201–211

Gabrié C (1998) ICRI (Initiative française pour les Récifs Coralliens). L'état des récifs coralliens en France Outre-Mer. Ministère de l'Aménagement du territoire et de l'Environnement, Secrétariat d'Etat à l'Outre-Mer, 136 pp

Garrigue C (1998) Distribution and biomass of microphytes measured by benthic in a tropical lagoon (New Caledonia, South Pacific). Hydrobiologia 385:1–10

Garrigues L, Deleersnijder E, Rancher J (1993) Modélisation bidimensionelle à deux couches de la circulation autour d'îles: Application aux atolls de Fangataufa et Mururoa. Service Mixte de Sécurité Radiologique, Commissariat à l'Energie Atomique et Ministère de la Défense, Dominiques

Gregoire M, Beckers JM, Nihoul JCJ, Stanev E (1998) Reconnaissance of the main Black Sea's ecohydrodynamics by means of a three-dimensional interdisciplinary model. J Mar Syst 16:85–105

Guarin F (1991) A model of the trophic structure of the soft-bottom community in Lingayen Gulf, Philippines: an application of the ECOPATH II software and modelling approach. Institute of Biology, College of Science, University of the Philippines, Quezon City. PhD Thesis, 75 pp

Hata H, Suzuki A, Maruyama T, kurano N, Miyachi S, Ikeda Y, Kayanne H (1998) Carbon flux by suspended and sinking particles around the barrier reef of Palau, western Pacific. Limnol Oceanogr 43(8):1883–1893

Hearn CJ, Holloway PE (1990) A three-dimensional barotropic model of the reponse of the Australian North West Shelf to tropical cyclones. J Phys Oceanogr 20:60–80

Henriksen K, Kemp WM (1988) Nitrogen cycling in coastal marine environments. Wiley, Chichester, 451 pp

Jarrige F, Radok R, Krause G, Rual P (1975) Courants dans le lagon de Nouméa, Nouvelle Calédonie. Déc 74–janv 75. Rapp ORSTOM (Nouméa) and H Lamb Inst of Oceanography, Flinders Univ, Adelaide, 6 pp

King B (1992) A predictive model of the currents in Cleveland Bay. In: Spaulding M, Bedford K, Blumberg A, Cheng R, Swanson C (eds) Estuarine and coastal modelling. ASCE, New York, pp 746–758

Koroleff F (1976) Determination of ammonia. In: Grasshoff K (ed) Methods of sea water analysis. Verlag Chemie, Weinheim, p 126–133

Kraines S, Suzuki A, Yanagi T, Isobe M, Guo X, Komiyama H (1999) Rapid water exchange between the lagoon and the open ocean at Majuro atoll due to wind, waves and tide. J Geophys Res C 104(7):15635–15653

Labrosse P, Fichez R, Farman R, Adams T, (2000) New Caledonia. In: Sheppard C (ed) Seas at the Millenium, an environmental evaluation, vol 2. Elsevier, Amsterdam, pp 723–736.

Langdon C (1993) The significance of respiration in production measurements based on oxygen. IECS Mar Sci Symp 197:69–78

Lazure P, Salomon J-C (1991) Coupled 2-D and 3-D modelling of coastal hydrodynamics. Oceanol Acta 14 (2):173–180

Le Borgne R, Rodier M, Le Bouteiller A, Kulbicki M (1997) Plankton biomass and production in an open atoll lagoon: Uvea, New Caledonia. J Exp Mar Biol Ecol 212:187–210

Leendertse JJ (1967) Aspects of a computational model for long-period water-wave propagation. Rand, Santa Monica, CA

McClanahan TR (1995) A Coral reef ecosystem-fisheries model: impacts of fishing intensity and catch selection on reef structure and processes. Ecol Model 80:1–19

Messinger F, Arakawa A (1976) Numerical methods used in atmospheric models, vol I. WMO, Geneva,64 pp

Morlière A (1985) Assainissement de Nouméa. Mesures de courant. ORSTOM, Noumea, 50 pp

Morlière A, Cremoux J-L (1981) Observations de courant dans le lagon, Février à Août 1981. ORSTOM, Noumea, 50 pp

Murphy J, Riley JP (1962) A modified single solution method for the determination of phosphate in natural waters. Anal Chim Acta 27:31–36

Nihoul JCJ (1984) A three-dimensional general marine circulation model in a remote sensing perspective. Ann Geophys 2:433–442

Niquil N, Jackson GA, Legendre L, Delesalle B (1998) Inverse model analysis of the planktonic food web of Takapoto Atoll (French Polynesia). Mar Ecol Prog Ser 165:17–29a

Peterson DH, Festa JF (1984) Numerical simulation of phytoplankton productivity in partially mixed estuarines. Estuar Coast Shelf Sci 19:563–589

Pinazo C, Marsaleix P, Millet B, Estournel C, Véhil R (1996) Spacial and temporal variability of phytoplancton biomass in upwelling areas of the northwestern Mediterranean: a coupled physical and biogeochemical modelling approach. J Mar Syst 7:161–191

Pinazo C, Marsaleix P, Millet B, Estournel C, Kondrachoff V, Véhil R (2001) Phytoplankton variability in summer in the northwestern Mediterranean: modelling of the wind and freshwater impacts. J Coast Res 17:146–161

Raimbault P, Slawyk G, Coste B, Fry J (1990) Feasibility of using an automatic colorimetric procedure for the determination of seawater nitrate in the 0 to 100 nM range: examples from field and culture. Mar Ecol Prog Ser 104:347–351

Raimbault P, Pouvesle W, Diaz F, Garcia N, Sempéré R (1999) Wet-oxidation and automated colorimetry for organic carbon, nitrogen and phosphorus dissolved in seawater. Mar Chem 66:161–169

Rancher J (1995) Courantologie à proximité des flancs et devant les passes des atolls de Mururoa et de Fangataufa. Service Mixte de Surveillance Radiologique et Biologique de l'homme et de l'environnement. Rapport N. 01-SMSRB-NP, Ministère de la Défense, Dominiques

Redfield AC, Ketchum BH, Richards FA (1963) The influence of organisms on the composition of seawater. In: The sea hill. Interscience, New York pp 26–77

Roman MR, Furnas MJ, Mullin MM (1990) Zooplankton abundance and grazing at Davies Reef, Great Barrier Reef, Australia. Mar Biol 105:73–82

Rougerie F (1986) Le lagon sud-ouest de Nouvelle Calédonie : spécificité hydrologique, dynamique et productivité. Etud Thèses, ORSTOM, Paris 231 pp

Ruddick KG, Deleersnijder E, Luyten PJ, Ozer J (1995) Haline stratification in the Rhine-Meuse plume: a three-dimensional model sensitivity analysis. Cont Shelf Res 15:1597–1630

Skliris N, Elkalay K, Goffart A, Frangoulis C, Hecq JH (2001) One-dimensional modelling of the plankton ecosytem of the north-western Corsican coastal area in relation to meteorological constraints. J Mar Syst 27:337–362

Skogen MD, Svendsen E, Berntsen J (1995) Modelling the primary production in the North Sea using a coupled three-dimensional physical-chemical-biological ocean model. Estuar Coast Shelf Sci 41(5):545–565

Smith SV (1984) Phosphorus versus nitrogen limitation in the marine environment. Limnol Oceanogr 9(6):1149–1160

Sorokin YI (1993) Coral reef ecology: ecological studies, vol 102. Springer-Verlag, Berlin, Heidelberg, New York, 465 pp

Steele JH (1962) Environmental control of photosynthesis in the sea. Limnol Oceanogr 7:137–150

Tartinville B, Deleersnijder E, Rancher J (1997) The water residence time in the Mururoa atoll lagoon: sensitivity analysis of a three-dimensional model. Coral Reefs 16:193–203

Testau JL, Conand F (1983) Estimation des surfaces des différentes zones du lagon de Nouvelle Calédonie. ORSTOM, Nouméa

Tett P (1990) A three layer vertical and microbiological processes model for shelf seas. Report No. 14, Proudman Oceanographic Laboratory, Birkenhead, 85 pp

Tett P, Grenz C (1994) Designing a simple microbiological-physical model for a coastal embayment. Vie Milieu 44(1):39–58

Torreton J-P, Pages J, Harris P, Talbot V, Pourlier S, Fichez R (1997) Eutrophisation en milieu lagonaire≫ Compte-Rendu, subvention CORDET N 94 T 09. ORSTOM, Tahiti

Tusseau-Vuillemin MH, Mortier L, Herbaut C (1998) Modelling nitrate fluxes in an open coastal environment (Gulf of Lions): transport versus biogeochemical processes. J Geophys Res 103 (C4):7693–7708

Von Arx Ws (1948) The circulation system of Bikini and Rongelap lagoons. Trans Am Geophys Union 29:861–870

Ward BB (2000) Nitrification and the marine nitrogen cycle. In: Kirchman DL (ed) Microbial ecology of the oceans. Wiley, New York, pp 427–453

Wolanski EJ (1994) Physical oceanographic processes of the Great Barrier Reef. CRC, Boca Raton, Florida, pp 1–194

Wolanski EJ, King B (1990) Flushing of Bowden Reef lagoon, Great Barrier Reef. Estuar Coast Shelf Sci 31:789–804

Young IR, Black KP, Heron ML (1994) Circulation in the Ribbon Reef region of the Great Barrier Reef. Cont Shelf Res 14:117–142

Yentsch CS, Menzel DW (1963) A method for the determination of phytoplankton chlorophyll and phaeophytin by fluorescence. Deep Sea Res 10:221–231

Zavatarelli M, Baretta JW, Baretta-Bekker JG, Pinardi N (2000) The dynamics of the Adriatic Sea ecosystem: an idealized model study. Deep Sea Res 47(5):937–970